Observational Study

Medicine

OPEN

High expression of KIF20A in bladder cancer as a potential prognostic target for poor survival of renal cell carcinoma

Bin Liu, MD[a,*], Jianzhi Su, MD[a], Bo Fan, MD[a], Xiaochen Ni, MD[a], Tingting Jin, MD[a]

Abstract

Urinary system tumors are malignant tumors, including renal cancer and bladder cancer. however, molecular target of them remains unclear. GSE14762 and GSE53757 were downloaded from GEO database to screen differentially expressed genes (DEGs). Weighted gene co-expression network analysis was performed. Gene Ontology (GO) and Kyoto encyclopedia of genes and genomes were used for enrichment analysis. Gene ontology and Kyoto encyclopedia of genes and genomes analyses were performed on whole genome, as formulated by gene set enrichment analysis. Survival analysis was also performed. Comparative toxicogenomics database was used to identify diseases most associated with hub genes. A total of 1517 DEGs were identified. DEGs were mainly enriched in cancer pathway, HIF-1 signaling pathway, organic acid metabolism, glyoxylate and dicarboxylate metabolism, and protein homodimerization activity. Ten hub genes (TPX2, ASPM, NUSAP1, RAD51AP1, CCNA2, TTK, PBK, MELK, DTL, kinesin family member 20A [KIF20A]) were obtained, which were up-regulated in tumor tissue. The expression of KIF20A was related with the overall survival of renal and bladder cancer. KIF20A was up-regulated in the tumor tissue, and might worsen the overall survival of bladder and kidney cancer. KIF20A could be a novel biomarker of bladder and kidney cancer.

Abbreviations: CTD = comparative toxicogenomics database, DEGs = differentially expressed genes, FDR = false discovery rate, GO = gene ontology, GSEA = gene set enrichment analysis, KEGG = Kyoto encyclopedia of genes and genomes, KIF20A = kinesin family member 20A, PPI = protein-protein interaction, WGCNA = weighted gene co-expression network analysis.

Keywords: bladder cancer, kidney cancer. prognostic targets, KIF20A, urinary system tumors

1. Introduction

Urinary system tumor is a disease that occurs frequently in urology.[1] Renal carcinoma also belongs to urinary system tumor,[2] there are no specific symptoms in initial clinical.[3] According to the epidemiological survey, the incidence of bladder cancer ranks fourth among all male malignant tumors worldwide.[4] With the increase of age of patients, the morbidity and mortality showed an increasing trend.[5] There may be a strong link between bladder cancer and renal cancer through genetic inheritance or target interaction.[6] However, the pathogenesis of bladder cancer and kidney cancer is unknown.[7] Previously, we identified PLK1 as research focus of bladder cancer,[8] and bioinformatic analysis showed that kinesin family member 20A (KIF20A) has a strong correlation with PLK1. Furthermore, we hypothesized that KIF20A might influence development of bladder and kidney cancer.

Bioinformatics technology, an interdisciplinary subject of biology and computer, and its research focus is mainly reflected in Genomics and Proteomics.[9] It can design drugs based on analyzing data such as DNA sequencing and functional genomes.[10]

KIF20A, protein coding gene located on chromosome 5q31.2, molecular weight of about 100kda.[11,12] KIF20A is involved in regulation of microtubule bundle formation, midbody separation and cytokinesis.[13] Pathways associated with KIF20A include cell cycle, mitosis, and responses to cytosolic Ca2 $^{+}$ elevation.[14] Gene ontology (GO) annotations linked to KIF20A included protein kinase binding and ATP hydrolysis activities.[15] However, mechanism of bladder cancer-related KIF20A in renal cancer is unknown.[16]

The paper analyzed renal cell carcinoma to obtain key genes, verify that high expression of KIF20A in bladder cancer may affect the survival rate of renal cancer, and verify KIF20A on renal cancer.

2. Method

2.1. Renal cancer dataset

Renal cancer data set GSE14762 and GSE53757 configuration file generated from GPL4866, GPL570 GEO database (http://www.ncbi.nlm.nih.gov/geo/). GSE14762 included 10 renal cancer and 12 normal tissue samples, GSE53757 included 72 renal cancer and 72 normal tissue samples to get differentially expressed genes (DEGs) in renal cancer.

The authors have no funding and conflicts of interest to disclose.

The datasets generated during and/or analyzed during the current study are publicly available.

[a] Department of Urology Surgery, The Fourth Hospital of Hebei Medical University, Hebei, PR China.

** Correspondence: Bin Liu, Department of Urology Surgery, The Fourth Hospital of Hebei Medical University, No.12 Jiankang Road, Hebei 050000, PR China (e-mail: liubinsy123@163.com).*

How to cite this article: Liu B, Su J, Fan B, Ni X, Jin T. High expression of KIF20A in bladder cancer as a potential prognostic target for poor survival of renal cell carcinoma. Medicine 2023;102:2(e32667).

Received: 15 November 2022 / Received in final form: 22 December 2022 / Accepted: 27 December 2022

http://dx.doi.org/10.1097/MD.0000000000032667

2.2. Go to batch processing

GSE14762 and GSE53757 were combined using R package in Silico Merging [DOD:10.1186/1471-2105-13-335] to obtain merge matrix. Furthermore, we used remove batch effect function of R package limma (version 3.42.2,) to remove batch effect, finally obtained matrix after removing batch effect, which was applied to subsequent analysis.

2.3. Screening of DEGs

R package "limma" was used for probe summary and background correction of merged matrices for GSE14762 and GSE53757. Used Benjamini-Hochberg method to set raw *P* values. Used fold change to get false discovery rate (FDR). Cutoff criterion for DEG was FDR < 0.05. Volcano plot was made, intersection DEGs were taken by Venn diagram.

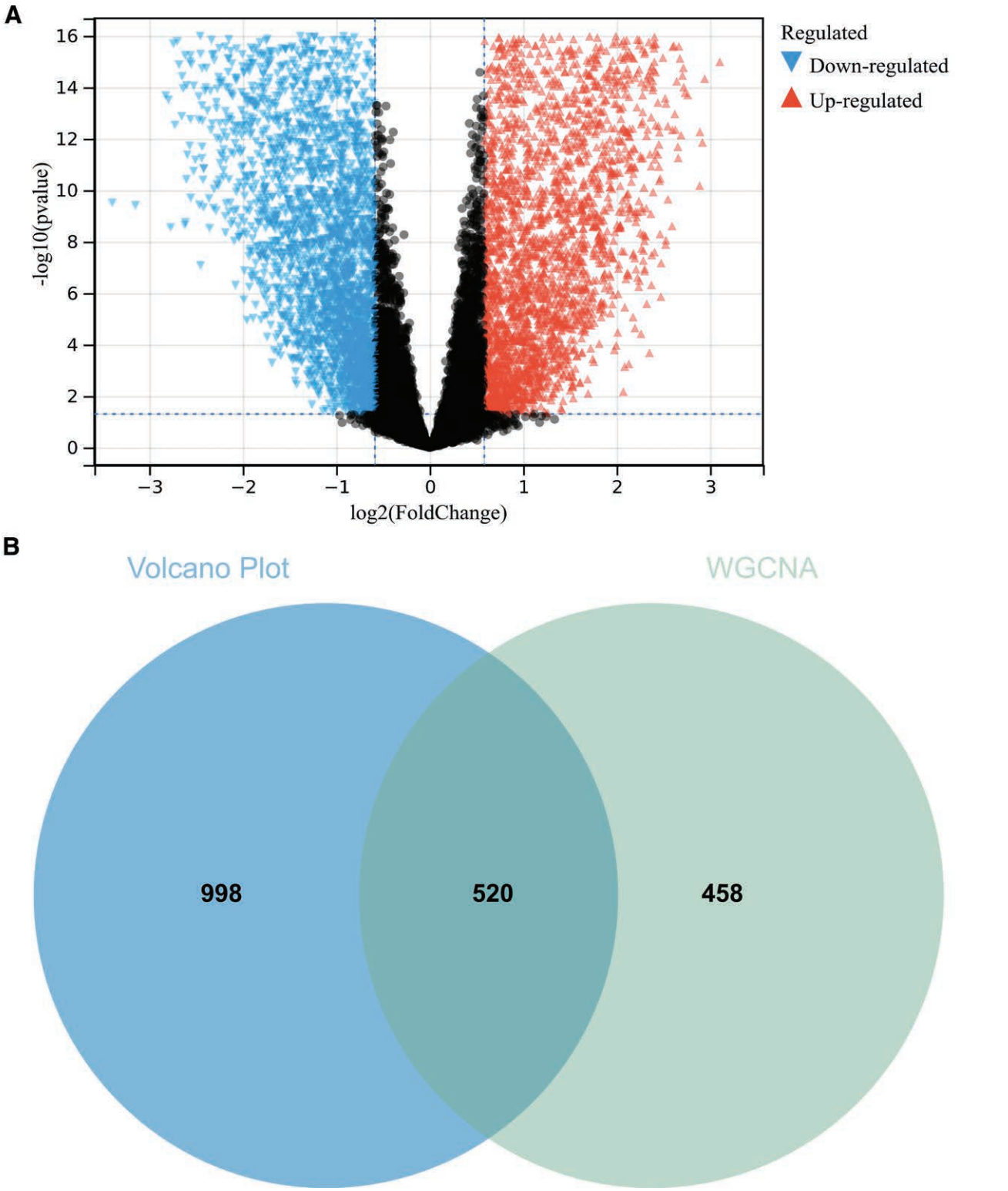

Figure 1. Analysis of differentially expressed genes. (A) 1517 DEGs were identified. Blue: Down-regulated; Red: Up-regulated (B) Draw Venn diagram and take intersection. DEGs = differentially expressed genes.

2.4. Weighted gene co-expression network analysis

We got Median Absolute Deviation of each gene separately by post-batch merging matrices of GSE14762 and GSE53757. For all genes in pairs perform Pearson correlation matrix and average chain method. using power function A_mn = | C_mn | ^β structure weighted adjacency matrix (C_mn = Pearson correlation between Gene_m and Gene_n; A_mn = adjacency between Gene m and Gene n). After selecting a power of 10, adjacency is

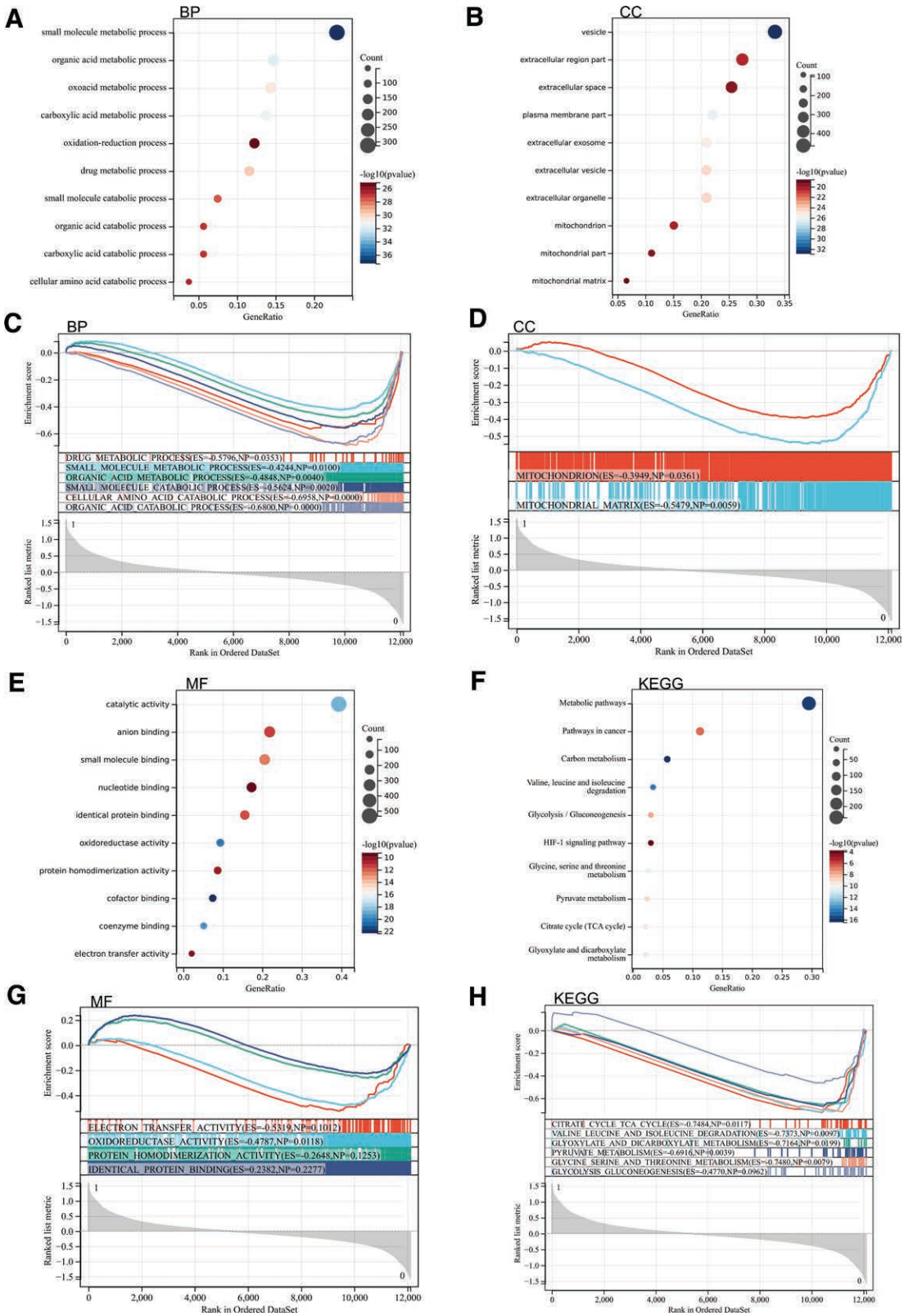

Figure 2. Functional enrichment analysis. (A, C, E, G) functional enrichment analysis of DEGs. (B, D, F, H) GSEA analysis. DEGs = differentially expressed genes, GSEA = gene set enrichment analysis.

transformed into a topological overlap matrix. Average linkage hierarchical clustering was performed, minimum size (genome) was 30. Sensitivity was set to 3. Calculated dissimilarity of module characteristic genes, selected a cut line for module dendrogram, merged some modules.

2.5. Protein-protein interaction (PPI) networks

The list of differential genes was input into the STRING (http://string db.org/) database to build a PPI network (confidence > 0.4) for predicting core genes. PPI network was imported into cytoscape software, module with best correlation was found by

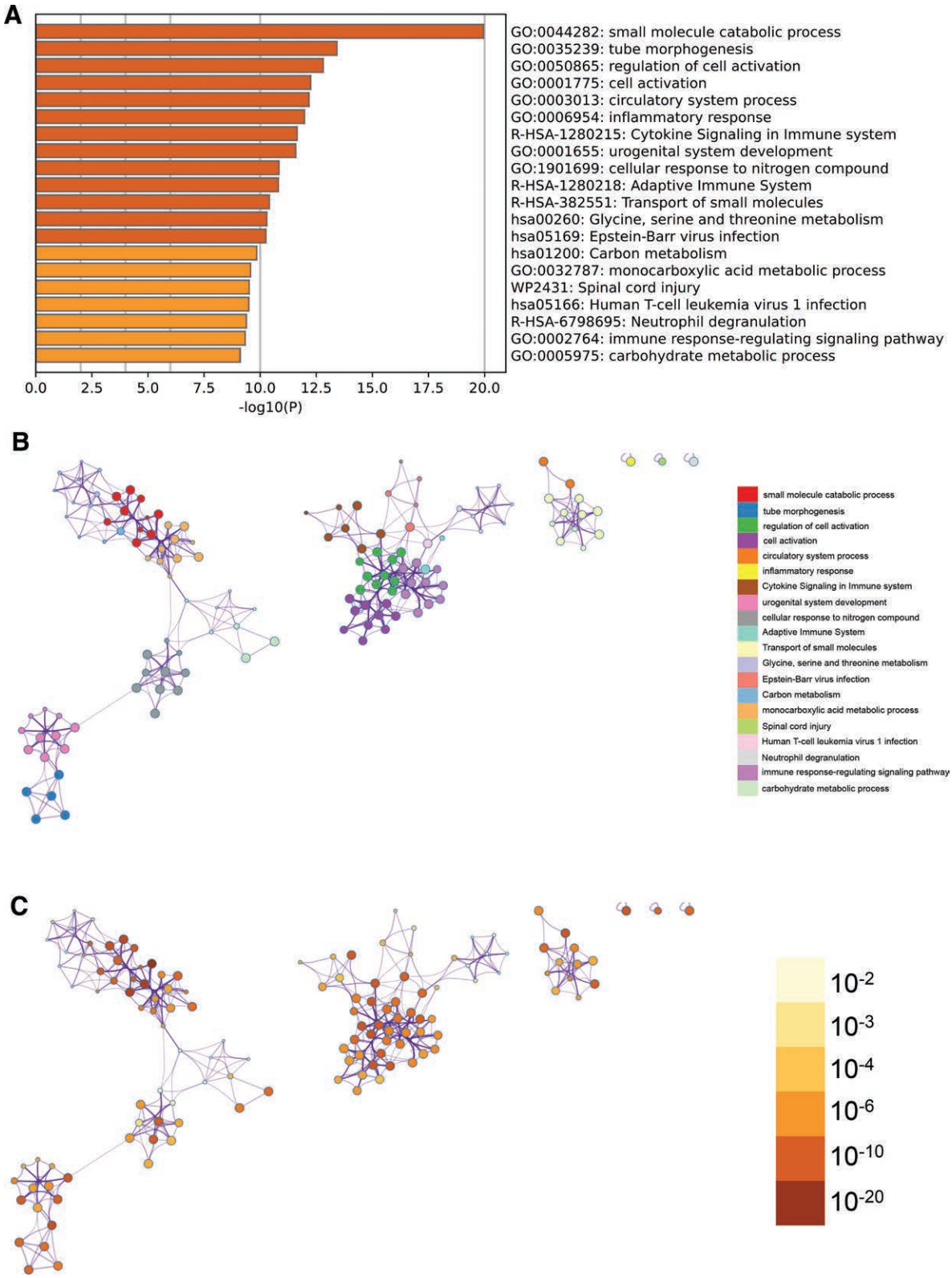

Figure 3. Enrichment analysis by Metascape. (A) GO analysis, (B) enriched networks colored by enriched terms and (C) enriched networks colored by *p*-values. GO = gene ontology.

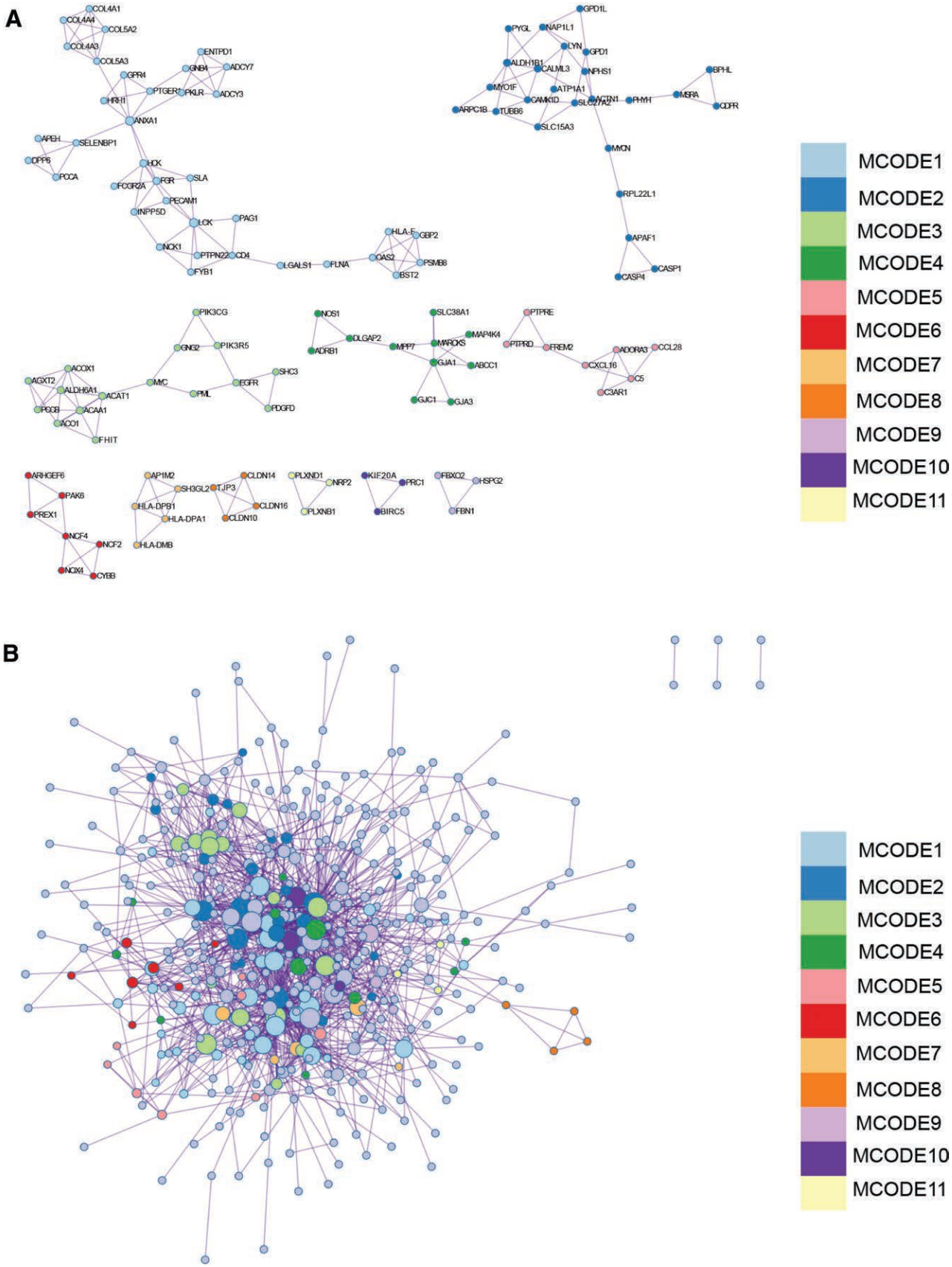

Figure 4. Enrichment analysis by Metascape.

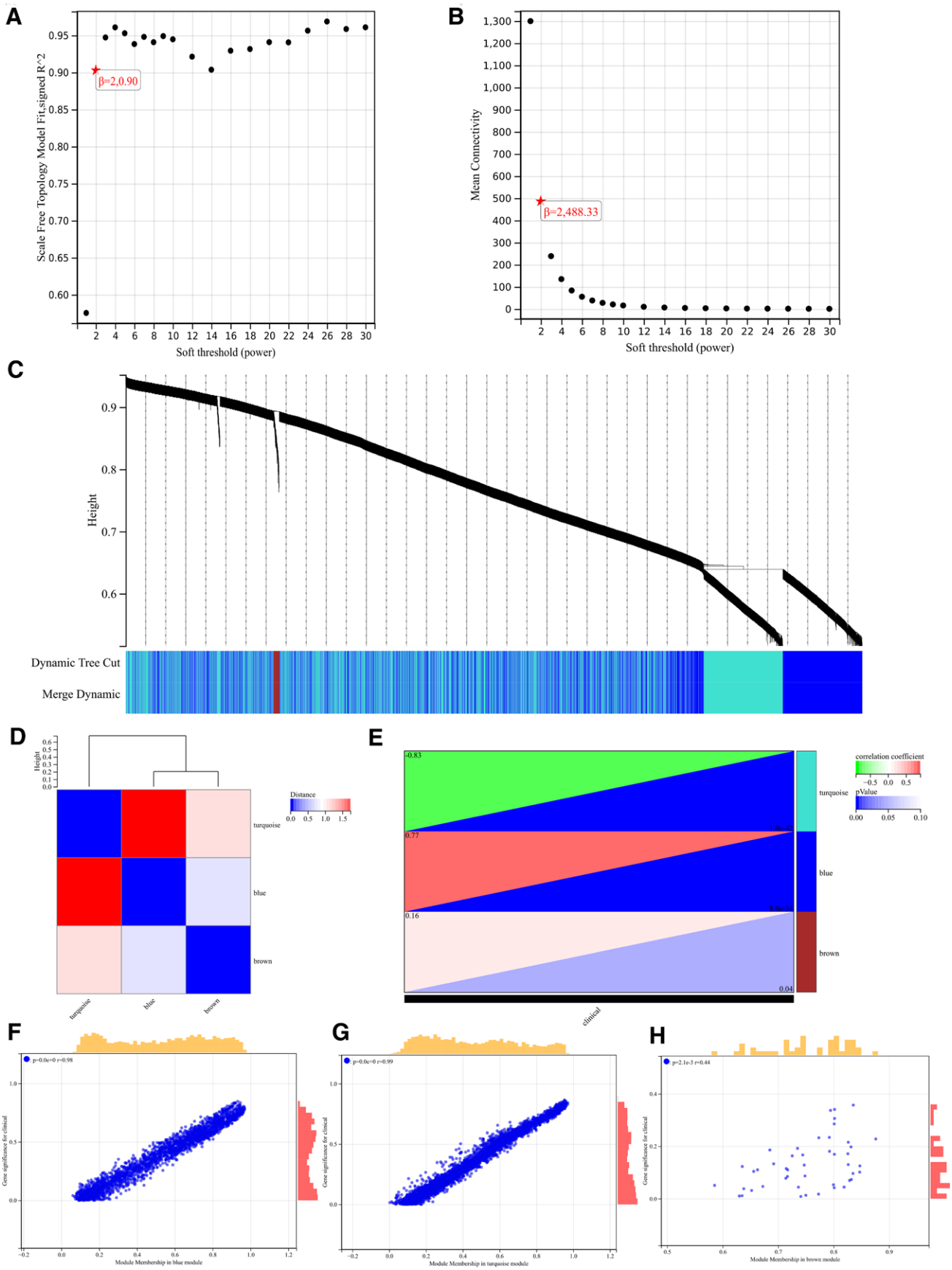

Figure 5. WGCNA analysis. (A) β = 2,0.90 (B) β = 2488.33. (C) Hierarchical clustering tree, which generated three important modules. (D) Interaction between modules. (E) Heatmap of correlation between modules and phenotypes (F–H) Scatter plot of correlation between GS and MM for related hub genes. WGCNA = weighted gene co-expression network analysis.

MCODE. Three algorithms (MCC, MNC, DMNC) were used to calculate 10 best correlation genes and take intersection, and core gene list was exported after visualization.

2.6. Functional enrichment analysis

This study will Wayne figure out the difference of gene list input Kyoto encyclopedia of genes and genomes (KEGG) rest

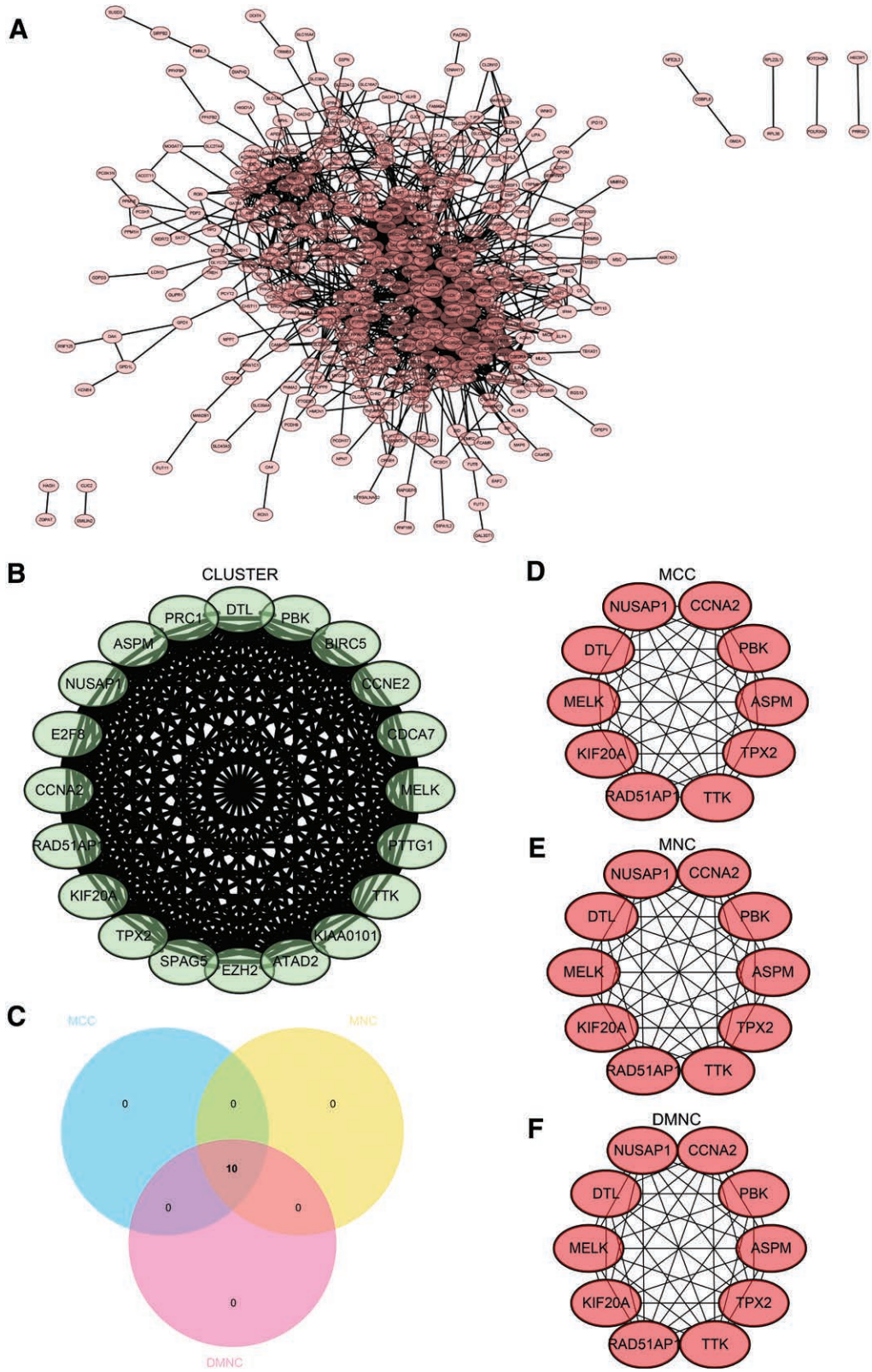

Figure 6. Construction and analysis of protein-protein interaction (PPI) networks. (A) PPI network of DEGs (B) core gene cluster (C) union was obtained by Venn diagram to obtain 10 core genes (D) MCC was used to identify central genes (E) MNC was used to identify central genes (F) DMNC was used to identify central genes. DEGs = differentially expressed genes, PPI = protein-protein interaction.

API (https://www.kegg.jp/kegg/rest/keggapi.html) to get latest KEGG Pathway gene annotation, Used R package cluster Profiler (version 3.14.3) for enrichment analysis to get results of gene set enrichment. GO annotation of genes in R software package org.Hs.e.g..db (version 3.1.0) was used as background, genes were mapped to background set. The minimum gene set was 5, maximum gene set was 5000. *P* value of < 0.05, FDR of < 0.25 were considered as measures of statistical significance.

In addition, we use Metascape database (http://metascape.org/gp/index.html), for above differences in gene enrichment of function analysis and export list.

2.7. Gene set enrichment analysis (GSEA) analysis

For GSEA, we derived from GSEA (DOI: 10.1073/ pnas.0506580102, http://software.broadinstitute.org/gsea/index.jsp) web site for GSEA software (version 3.0). Samples were divided into 2 groups based on renal cancer and normal tissue and derived from Molecular Signatures Database (DOI: 10.1093/ bioinformatics/btr260, http://www.gsea-msigdb.org/gsea/downloads.jsp) to download c2.cp.kegg.v7.4.symbols.gmt. Based on gene expression profile and phenotype grouping, a minimum gene set of 5, a maximum gene set of 5000, 1000 resampling.

2.8. Heat map of gene expression

By R package heatmap to make a heatmap of expression degree of core genes found by the 2 algorithms in PPI network in GSE14762 and GSE53757 visually displayed expression differences of core genes between renal cancer and normal tissue.

2.9. Survival analysis

We obtained clinical survival data and corresponding gene expression data from TCGA to verify whether the core genes had predictive power in survival. Used R software package maxstat (version:0.7–25) to calculate optimal cutoff value of Risk Score of 10 core genes, best cutoff value is calculated, Survfit function of the R package survival was further used to find prognostic differences. We also used R package forest to make a forest map of 10 core genes to observe whether each independent core gene had a significant effect on prognosis of renal cancer.

2.10. Comparative toxicogenomics database (CTD) analysis

We entered the core genes into CTD website, found most relevant diseases to core genes, used Excel to draw differential expression radar map for each gene.

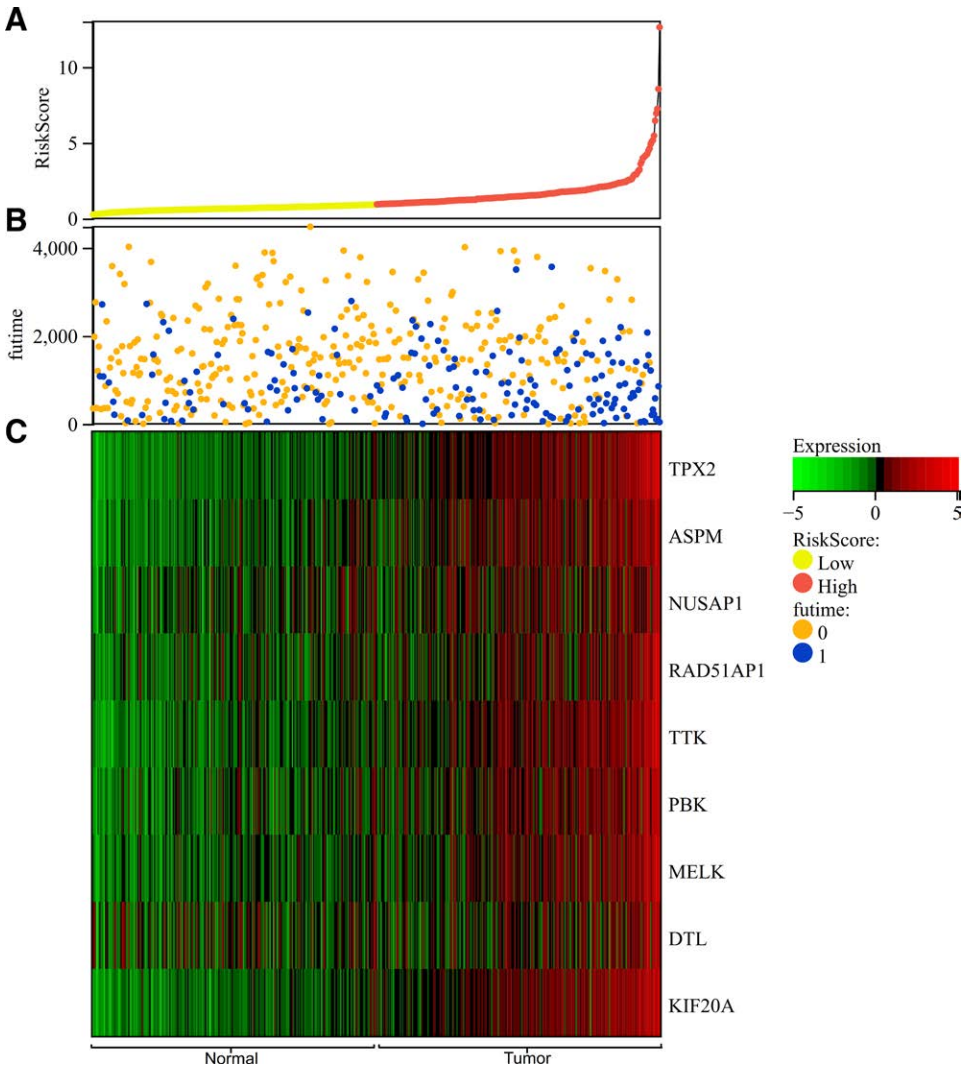

Figure 7. Prognostic score relationship and gene expression heat map. (A, B) The survival time and survival rate of the low-risk group were significantly higher than those of the high-risk group. (C) 10 core genes (TPX2, ASPM, NUSAP1, RAD51AP1, CCNA2, TTK, PBK, MELK, DTL, KIF20A) were obtained with high expression in tumor tissue samples and low expression in normal tissue samples. KIF20A = Kinesin family member 20A.

2.11. RT-qPCR assay

Homogenize tissue samples in 1 ml of RNA Extraction per 20 mg of tissue using power homogenizer. The sample volume should not exceed 10% of the volume of RNA Extraction used for the homogenization.

After thawing, mix and briefly centrifuge the components of the kit. Add the following reagents into a sterile, nuclease-free tube on ice in the indicated order:

Template RNA 2 μg, Primer Oligo (dT) 18 primer 0.5 μL and Random Hexamer primer 0.5 μL or gene-specific primer 1 μL, 5X Reaction Buffer 4 μL, Servicebio®RT Enzyme Mixa 1 μL, Water, nuclease-free to 20 μL, Total volume 20 μL. Incubate for 5 minutes at 25°C, 30 minutes at 42°C. Terminate the reaction by heating at 85°C for 5 seconds.

The results of processing:

ΔΔCT method:

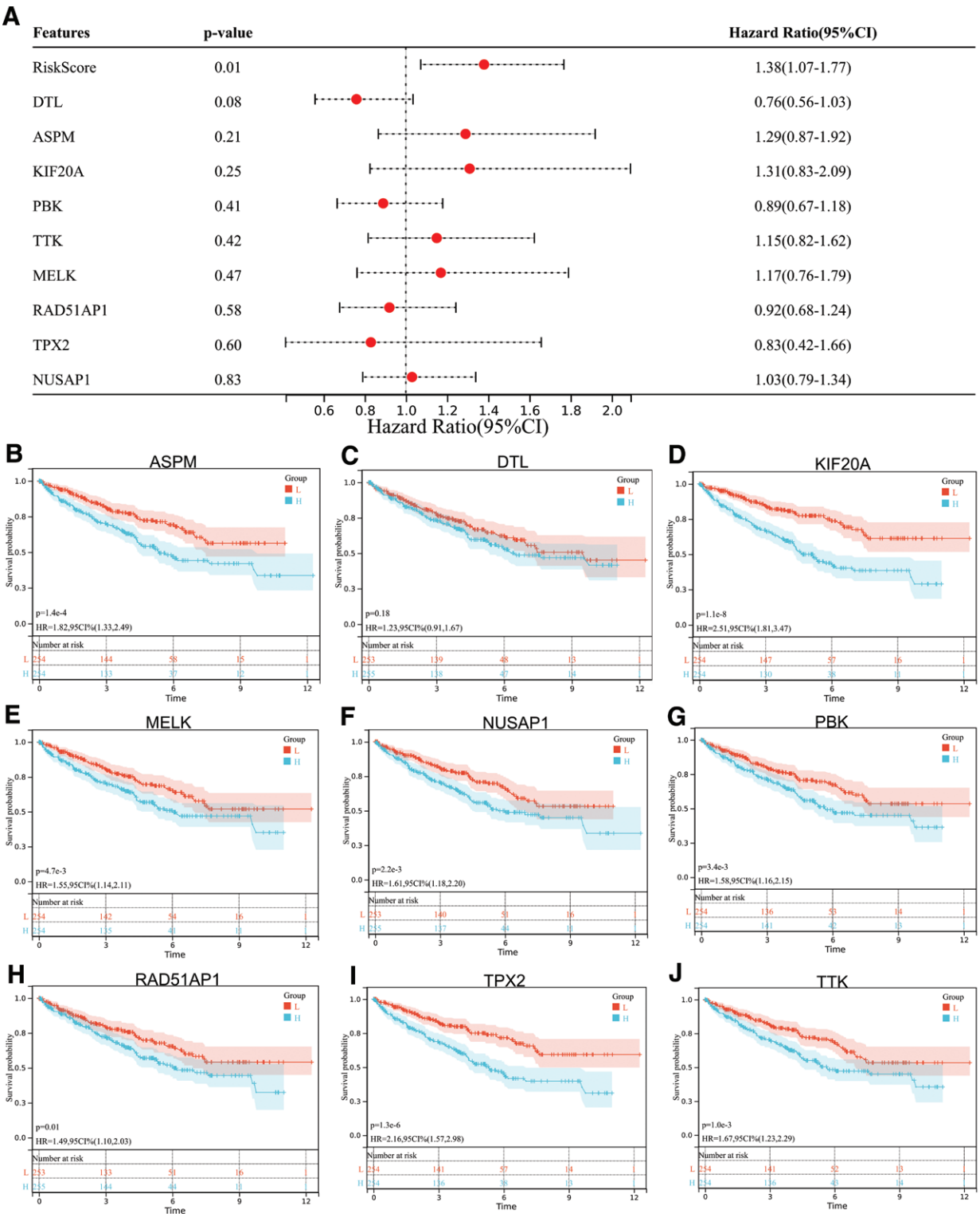

Figure 8. Survival analysis. (A) Forest plot of core genes (TPX2, ASPM, NUSAP1, RAD51AP1, CCNA2, TTK, PBK, MELK, DTL, KIF20A) related to renal cancer (B–J) survival curves of the 10 core genes. KIF20A = Kinesin family member 20A.

A = CT (target gene, sample) - CT (internal standard gene, sample)
B = CT (target gene, control) - CT (internal standard gene, control)
K = A to B
RNA Expression = 2^{-K}
The primer of KIF20A:
Forward Primer: TCTGTCGTCTCTACCTCCCTA
Reverse Primer: CAAGGGCCTAACCCTCAAGTA

3. Results

3.1. Differential gene analysis

1517 DEGs were found based on DEGs identified in debatching merge matrix of GSE14762 and GSE53757 (Fig. 1A).

3.2. Functional enrichment analysis

3.2.1. Functional enrichment analysis of DEGs. In GO analysis, they were mostly concentrated in organic acid metabolic process, metabolic pathway, cancer pathway, HIF-1 signaling pathway, glyoxylate and dicarboxylate metabolism, protein homodimerization activity (Fig. 2A, C, E, G).

3.2.2. GSEA analysis. GSEA enrichment analysis terms were similar to GO and KEGG enrichment terms of DEGs, which were mostly concentrated in organic acid metabolism, glyoxylate and dicarboxylate metabolism, protein homodimerization activity (Fig. 2B, D, F, H).

3.2.3. Enrichment analysis by Metascape. Among the enrichment items of Metascape, GO has inflammatory response, cytokine signaling in the immune system, immune response regulation signaling pathways (Fig. 3A), and has enrichment networks colored by enrichment terms and *p*-values (Fig. 3B, C, Fig. 4).

3.2.4. Weighted gene co-expression network analysis (WGCNA) analysis. Soft threshold power in WGCNA analysis was set to 9, which is lowest power for a scale-free topological fit index of 0.9 (Fig. 5A, B). Hierarchical clustering trees were constructed for all genes and yielded 3 significant modules (Fig. 5C). Interactions between these modules were then analyzed (Fig. 5D). Heatmaps of correlation between modules and phenotypes (Fig. 5E) and scatter plots of correlation between GS and MM for related hub genes (Fig. 5F–H) were also generated.

We calculated module characteristic vector correlation with expression of genes for MM, according to cutting standard (|MM| > 0.8), in clinical significant module has 3 high connectivity gene was identified as hub. We also drew a Venn diagram by WGCNA with differential genes screened by DEGs and took intersection (Fig. 1B)

3.3. Protein-protein interaction networks

Analyzed by Cytoscape software (Fig. 6A) to obtain core gene clusters (Fig. 6B). Three different algorithms were used to confirm core genes (Fig. 6D–F). Venn diagram was used to obtain union (Fig. 6C), which resulted in 10 core genes (TPX2, ASPM, NUSAP1, RAD51AP1, CCNA2, TTK, PBK, MELK, DTL, KIF20A).

3.4. Prognostic score relationship and gene expression heat map

We found survival time and survival rate were significantly higher in low-risk group than in high-risk group (Fig. 7A, B). We

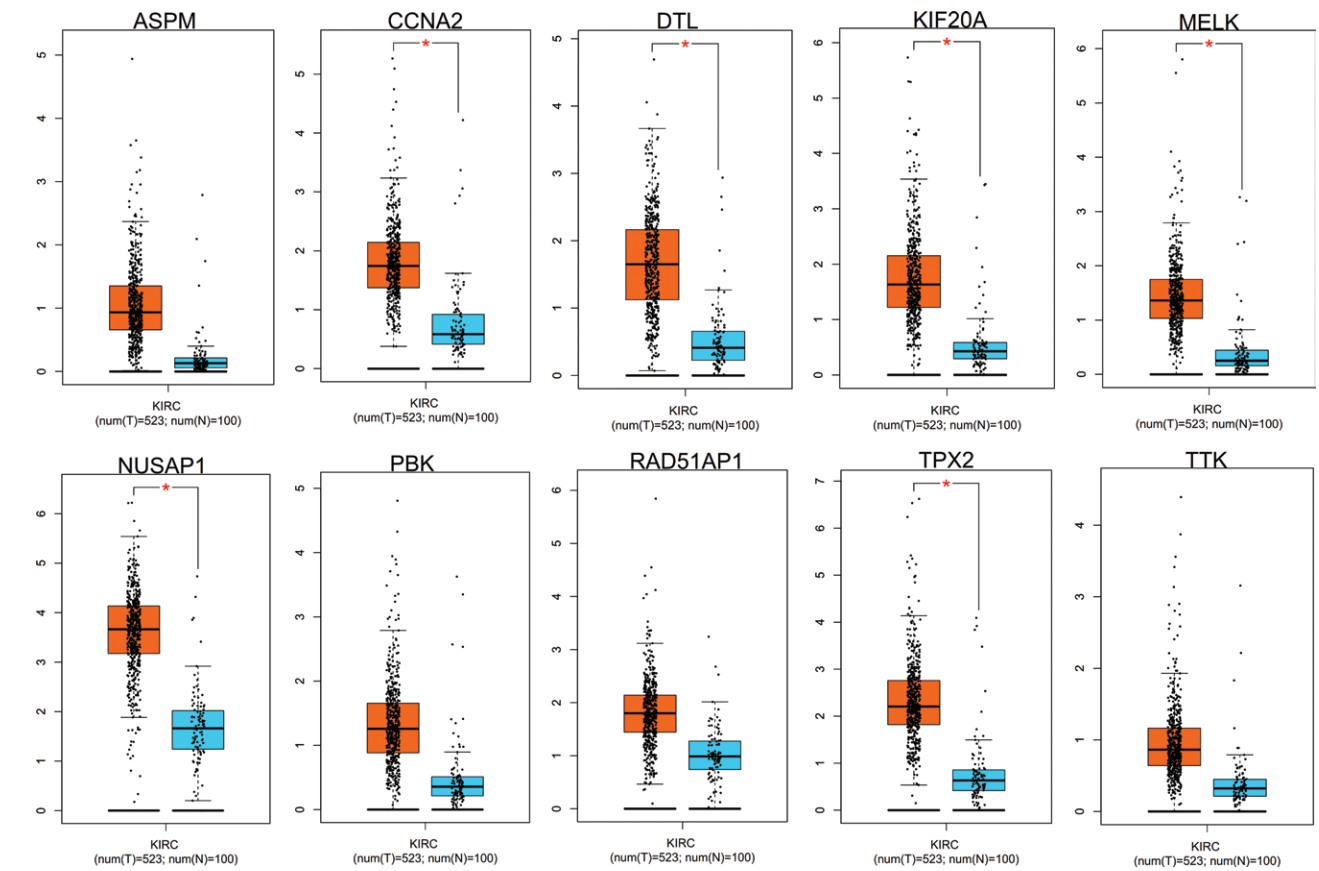

Figure 9. Box plot of core genes in renal cell carcinoma.

obtained 10 core genes (TPX2, ASPM, NUSAP1, RAD51AP1, CCNA2, TTK, PBK, MELK, DTL, KIF20A) and found that these core genes were highly expressed in tumor tissue samples and poorly expressed in normal tissue samples (Fig. 7C).

3.5. Survival analysis

We obtained forest plots of core genes (TPX2, ASPM, NUSAP1, RAD51AP1, CCNA2, TTK, PBK, MELK, DTL, KIF20A) associated with renal cancer (Fig. 8A) and survival plots of the 10 core

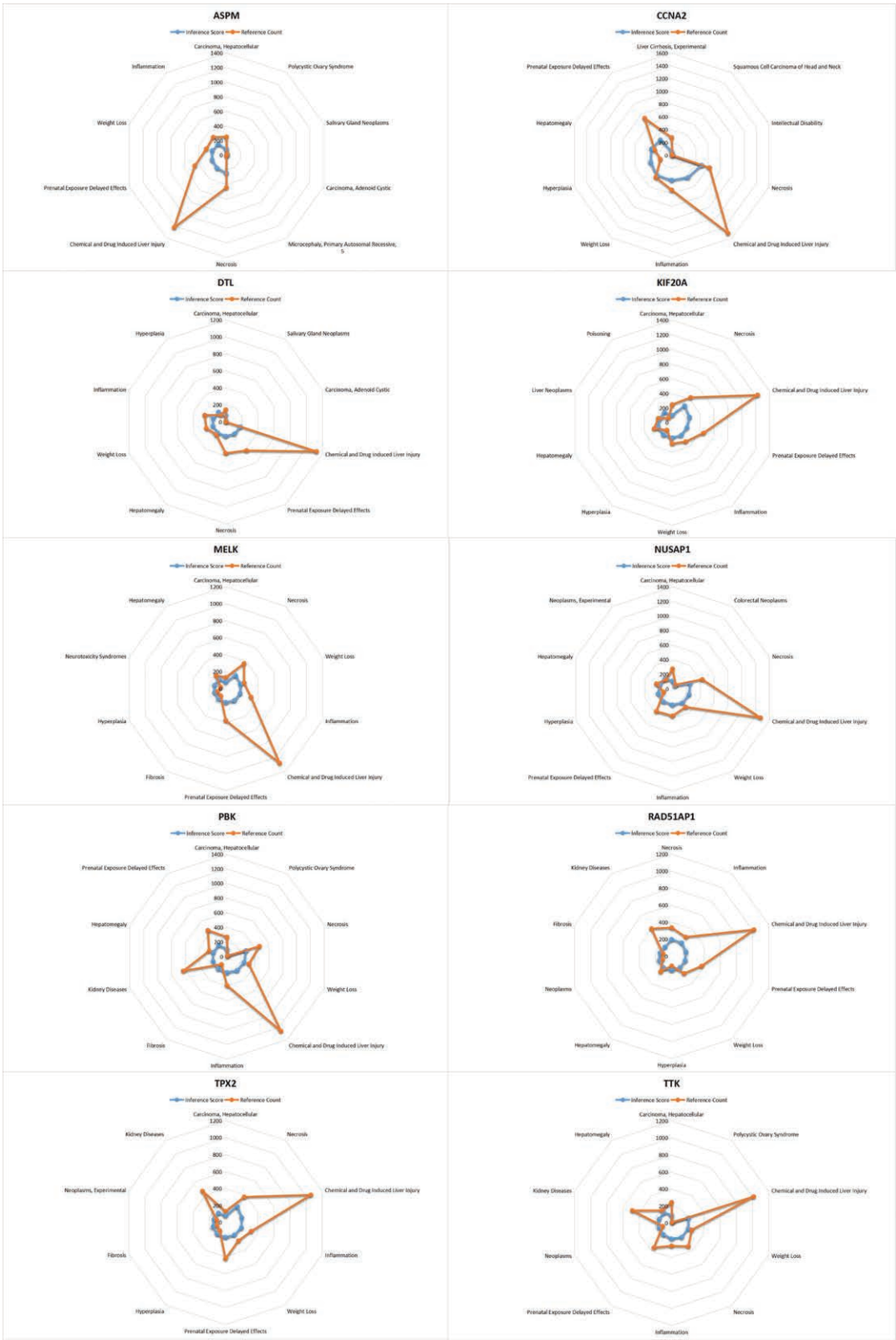

Figure 10. CTD analysis. 10 genes (TPX2, ASPM, NUSAP1, RAD51AP1, CCNA2, TTK, PBK, MELK, DTL, KIF20A) were related to necrosis, inflammation, adenoid cystic carcinoma, kidney disease, and tumor. CTD = comparative toxicogenomics database, KIF20A = Kinesin family member 20A.

genes (Fig. 8B–J). Box plots of core genes in renal carcinoma were also obtained (Fig. 9).

3.6. CTD analysis

We found 10 genes (TPX2, ASPM, NUSAP1, RAD51AP1, CCNA2, TTK, PBK, MELK, DTL, KIF20A) were linked to necrosis, inflammation, adenoid cystic carcinoma, renal disease, and tumor. (Fig. 10)

3.7. The correlation between PLK1 and KIF20A in the bladder cancer

There was strong correlation between PLK1 and KIF20A in the bladder cancer ($R = 0.65$, $P < .001$) (Fig. 11A). Compared with the normal tissue, the expression of KIF20A was higher expression in the bladder cancer (Fig. 11B).

3.8. The expression of KIF20A via the RT-PCR

Compared with the normal tissues, the expression of KIF20A was up-regulated in the bladder cancer through the RT-PCR ($P < .05$, Fig. 12)

4. Discussion

The main symptoms of urinary system tumors were frequent urination, hematuria, urgency, dysuria, abdominal pain, etc. The typical manifestation was painless and progressive gross hematuria. Bladder cancer is very harmful, which can cause fibrosis of the bladder, reduce the capacity of the bladder, and even reflux of the ureter and urine. It is also invasive and metastatic, which can endanger life and even lead to death.[17] One of most common hazards of renal cell carcinoma is hematuria. There may also be fever, anemia, hypertension, cachexia, metastatic symptoms of other sites, and bone pain.[18] We found KIF20A is highly expressed in bladder cancer, also highly expressed in renal cancer, and resulted in a poor survival prognosis of renal cancer patients.

KIF20A is 1 of motor protein-6 subfamily, mainly responsible for regulating intracellular motility and cell division.[19–22] KIF20A is a microtubule-associated motor protein, generating mechanical forces through coupling to adenosine triphosphate hydrolysis that are central to mitosis and cytokinesis.[23–26] KIF20A cross-links plasma membrane to microtubule cytoskeleton, which in turn promotes establishment of intracellular Bridges,[27] also preventing cross-linking and unpolymerization of cytoplasmic microtubules.[28]

KIF20A and other kinesin mitosis might be in cell fate determination factor is very important for transportation, may leading to cell division symmetrical or asymmetrical results.[29–34]

KIF20A is an important regulator of cytokinesis.[35,36] There is evidence that KIF20A linked to cancer.[37,38] Related studies have shown that ARAP1-AS1 regulates expression of KIF20A by infiltrating miR-3918, thereby helping bladder cancer cells activity,[39] affecting survival level of bladder cancer.[16] KIF20A is also responsible for intracellular trafficking of vesicles and organelles, and cell mitotic spindle formation.[40–44]

KIF20A can encode a mitogenic kinesin-like molecule with ATP activity that can move toward the microtubule anode. The gene functions as a microtubule-associated motor protein at telophase of meiosis and is also involved in mediating the transport of vesicles.[45,46] Abnormal expression of KIF20A is associated with chromosomal instability. It has been shown that KIF20A accumulates in the nucleus during the G2 phase of the cell cycle, leading to enhanced proliferation of pathological cells.[47] Xu's research found that the KIF20A was 1 hub biomarker of renal cancer, and identified as an independent RCC prognostic factor.[48]

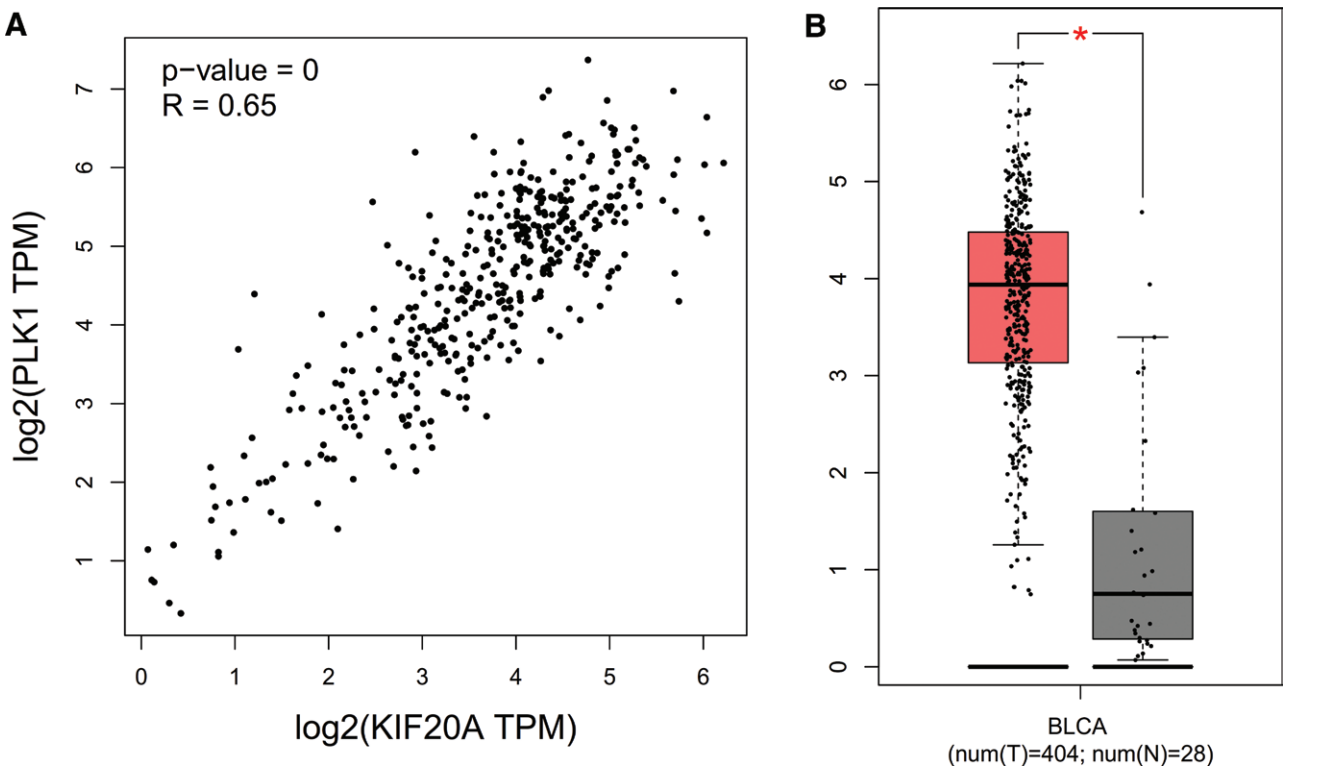

Figure 11. The role of PLK1 and KIF20A in the bladder cancer. (A) The strong correlation between PLK1 and KIF20A in the bladder cancer. (B) The expression of KIF20 A in the bladder cancer tissues. Compared with the normal tissue, the expression of KIF20A was higher expression in the bladder cancer. KIF20A = Kinesin family member 20A.

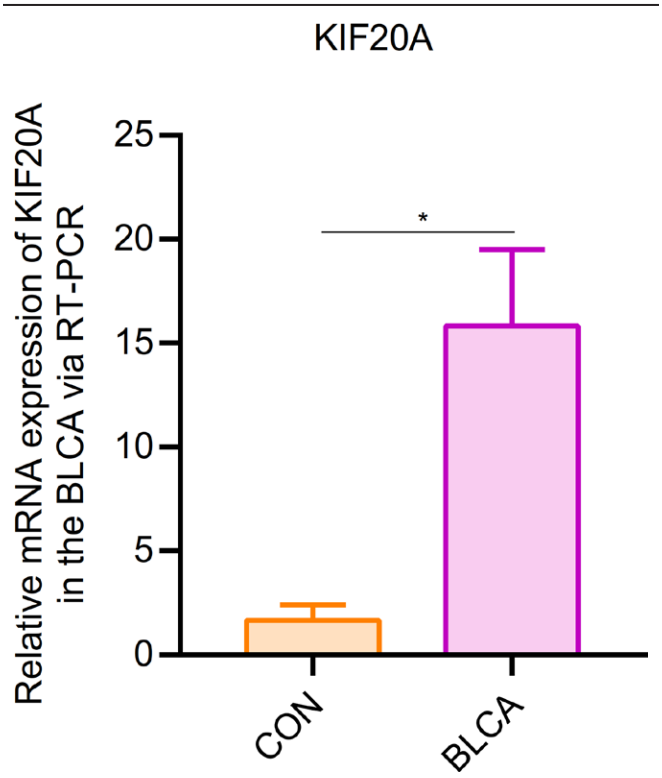

Figure 12. The status of KIF20A in bladder cancer tissue and confirm that the expression is higher when compared to normal tissue by PCR. KIF20A = Kinesin family member 20A.

KIF20A is important for immune cell infiltration. KIF20A increased infiltration levels of *T* cells follicular helper and *T* cells regulatory (Tregs).[48,49] KIF20A is overexpressed in many types of tumors,[15] it is related to occurrence of tumors, which is a stimulating factor for their malignant phenotype.[50] KIF20A may also be a useful biomarker in progression of nasopharynx cancer.[51] KIF20A can help colorectal cancer cells become active and enhances their resistance to chemotherapy by regulating JAK/STAT3 signaling pathway.[52] KIF20A levels affect sensitivity of hepatoma cells to chemotherapy drugs, have better prognosis.[53] KIF20A also have abnormal performance in prostate cancer.[54] KIF20A promotes fibrosarcoma development through PI3K-Akt signaling pathway.[55] Combine the above survey results, it is possible that KIF20A has a certain effect on renal cell carcinoma.

Our investigation also has some shortcomings, we have not conducted animal studies on expression or knockout to support it. We should go into more exploration of this later. KIF20A gene may be an important factor affecting renal cancer.

Author contributions

Conceptualization: Bin Liu.
Data curation: Jianzhi Su.
Formal analysis: Jianzhi Su.
Investigation: Jianzhi Su.
Methodology: Jianzhi Su, Bo Fan.
Project administration: Bin Liu, Bo Fan.
Resources: Bo Fan, Xiaochen Ni.
Software: Bo Fan, Tingting Jin.
Supervision: Xiaochen Ni, Tingting Jin.
Validation: Xiaochen Ni, Tingting Jin.
Visualization: Tingting Jin.
Writing – original draft: Bin Liu.
Writing – review & editing: Bin Liu, Tingting Jin.

References

[1] Karaosmanoglu AD, Onur MR, Karcaaltincaba M, et al. Secondary tumors of the urinary system: an imaging conundrum. Korean J Radiol. 2018;19:742–51.
[2] Raza SA, Jhaveri KS. MR imaging of urinary bladder carcinoma and beyond. Radiol Clin North Am. 2012;50:1085–110.
[3] Gray RE, Harris GT. Renal cell carcinoma: diagnosis and management. Am Fam Physician. 2019;99:179–84.
[4] Seidl C. Targets for therapy of bladder cancer. Semin Nucl Med. 2020;50:162–70.
[5] Ahmadi H, Duddalwar V, Daneshmand S. Diagnosis and staging of bladder cancer. Hematol Oncol Clin North Am. 2021;35:531–41.
[6] Scholtes MP, Alberts AR, Iflé IG, et al. Biomarker-oriented therapy in bladder and renal cancer. Int J Mol Sci. 2021;22.
[7] Suarez-Ibarrola R, Hein S, Reis G, et al. Current and future applications of machine and deep learning in urology: a review of the literature on urolithiasis, renal cell carcinoma, and bladder and prostate cancer. World J Urol. 2020;38:2329–47.
[8] Liu B, Meng LB, Su JZ, et al. PLK1 as one novel target for the poor prognosis of bladder cancer: an observational study. Medicine (Baltim). 2022;101:e30723e30723.
[9] Wang Y, Zhao Y, Bollas A, et al. Nanopore sequencing technology, bioinformatics and applications. Nat Biotechnol. 2021;39:1348–65.
[10] Chen J, Zhang Y, Shen B. Bioinformatics for the origin and evolution of viruses. Adv Exp Med Biol. 2022;1368:53–71.
[11] Echard A, Jollivet F, Martinez O, et al. Interaction of a Golgi-associated kinesin-like protein with Rab6. Science. 1998;279:580–5.
[12] Lai F, Fernald AA, Zhao N, et al. cDNA cloning, expression pattern, genomic structure and chromosomal location of RAB6KIFL, a human kinesin-like gene. Gene. 2000;248:117–25.
[13] Liang B, Zhou Y, Jiao J, et al. Integrated analysis of transcriptome data revealed AURKA and KIF20A as critical genes in medulloblastoma progression. Front Oncol. 2022;12:875521.
[14] Ren X, Chen X, Ji Y, et al. Upregulation of KIF20A promotes tumor proliferation and invasion in renal clear cell carcinoma and is associated with adverse clinical outcome. Aging (Albany NY). 2020;12:25878–94.
[15] Sheng Y, Wang W, Hong B, et al. Upregulation of KIF20A correlates with poor prognosis in gastric cancer. Cancer Manag Res. 2018;10:6205–16.
[16] Shen T, Yang L, Zhang Z, et al. KIF20A affects the prognosis of bladder cancer by promoting the proliferation and metastasis of bladder cancer cells. Dis Markers. 2019;2019:14863182–9.
[17] Lenis AT, Lec PM, Chamie K, et al. Bladder cancer: a review. JAMA. 2020;324:1980–91.
[18] Yong C, Stewart GD, Frezza C. Oncometabolites in renal cancer. Nat Rev Nephrol. 2020;16:156–72.
[19] Nguyen PA, Groen AC, Loose M, et al. Spatial organization of cytokinesis signaling reconstituted in a cell-free system. Science. 2014;346:244–7.
[20] Cesario JM, Jang JK, Redding B, et al. Kinesin 6 family member subito participates in mitotic spindle assembly and interacts with mitotic regulators. J Cell Sci. 2006;119(Pt 22):4770–80.
[21] Hirokawa N, Noda Y, Tanaka Y, et al. Kinesin superfamily motor proteins and intracellular transport. Nat Rev Mol Cell Biol. 2009;10:682–96.
[22] Geng A, Qiu R, Murai K, et al. KIF20A/MKLP2 regulates the division modes of neural progenitor cells during cortical development. Nat Commun. 2018;9:2707.
[23] Hirokawa N, Noda Y, Okada Y. Kinesin and dynein superfamily proteins in organelle transport and cell division. Curr Opin Cell Biol. 1998;10:60–73.
[24] Exertier P, Javerzat S, Wang B, et al. Impaired angiogenesis and tumor development by inhibition of the mitotic kinesin Eg5. Oncotarget. 2013;4:2302–16.
[25] Mandal K, Pogoda K, Nandi S, et al. Role of a Kinesin motor in cancer cell mechanics. Nano Lett. 2019;19:7691–702.
[26] She ZY, Li YL, Lin Y, et al. Kinesin-6 family motor KIF20A regulates central spindle assembly and acrosome biogenesis in mouse spermatogenesis. Biochim Biophys Acta Mol Cell Res. 2020;1867:118636.
[27] Fung S, Kitagawa M, Liao PJ, et al. Opposing activities of aurora B kinase and B56-PP2A phosphatase on MKlp2 determine abscission timing. Curr Biol. 2017;27:78–86.
[28] Fontijn RD, Goud B, Echard A, et al. The human kinesin-like protein RB6K is under tight cell cycle control and is essential for cytokinesis. Mol Cell Biol. 2001;21:2944–55.
[29] Qiu R, Wang J, Tsark W, et al. Essential role of PDZ-RGS3 in the maintenance of neural progenitor cells. Stem Cells. 2010;28:1602–10.

[30] Kawai Y, Shibata K, Sakata J, et al. KIF20A expression as a prognostic indicator and its possible involvement in the proliferation of ovarian clear-cell carcinoma cells. Oncol Rep. 2018;40:195–205.
[31] Atherton J, Yu IM, Cook A, et al. The divergent mitotic kinesin MKLP2 exhibits atypical structure and mechanochemistry. Elife. 2017;6.
[32] Janisch KM, McNeely KC, Dardick JM, et al. Kinesin-6 KIF20B is required for efficient cytokinetic furrowing and timely abscission in human cells. Mol Biol Cell. 2018;29:166–79.
[33] Adams RR, Carmena M, Earnshaw WC. Chromosomal passengers and the (aurora) ABCs of mitosis. Trends Cell Biol. 2001;11:49–54.
[34] D'Avino PP, Savoian MS, Glover DM. Cleavage furrow formation and ingression during animal cytokinesis: a microtubule legacy. J Cell Sci. 2005;118(Pt 8):1549–58.
[35] Zhao X, Zhou LL, Li X, et al. Overexpression of KIF20A confers malignant phenotype of lung adenocarcinoma by promoting cell proliferation and inhibiting apoptosis. Cancer Med. 2018;7:4678–89.
[36] Lee SH, McCormick F, Saya H. Mad2 inhibits the mitotic kinesin MKlp2. J Cell Biol. 2010;191:1069–77.
[37] Khongkow P, Gomes AR, Gong C, et al. Paclitaxel targets FOXM1 to regulate KIF20A in mitotic catastrophe and breast cancer paclitaxel resistance. Oncogene. 2016;35:990–1002.
[38] Ferrero H, Corachán A, Quiñonero A, et al. Inhibition of KIF20A by BKS0349 reduces endometriotic lesions in a xenograft mouse model. Mol Hum Reprod. 2019;25:562–71.
[39] Zhang W, Zhang J, Hu Z, et al. LncRNA ARAP1-AS1 promotes bladder cancer development by regulating the miR-3918/KIF20A axis. Mol Biotechnol. 2022;64:1259–69.
[40] Verhey KJ, Hammond JW. Traffic control: regulation of kinesin motors. Nat Rev Mol Cell Biol. 2009;10:765–77.
[41] Goldstein LS, Philp AV. The road less traveled: emerging principles of kinesin motor utilization. Annu Rev Cell Dev Biol. 1999;15:141–83.
[42] Neef R, Gruneberg U, Kopajtich R, et al. Choice of Plk1 docking partners during mitosis and cytokinesis is controlled by the activation state of Cdk1. Nat Cell Biol. 2007;9:436–44.
[43] Lai F, Godley LA, Joslin J, et al. Transcript map and comparative analysis of the 1.5-Mb commonly deleted segment of human 5q31 in malignant myeloid diseases with a del (5q). Genomics. 2001;71:235–45.
[44] Neef R, Grüneberg U, Barr FA. Assay and functional properties of rabkinesin-6/Rab6-KIFL/MKlp2 in cytokinesis. Methods Enzymol. 2005;403:618–28.
[45] Vale RD, Reese TS, Sheetz MP. Identification of a novel force-generating protein, kinesin, involved in microtubule-based motility. Cell. 1985;42:39–50.
[46] Hirokawa N, Noda Y. Intracellular transport and kinesin superfamily proteins, KIFs: structure, function, and dynamics. Physiol Rev. 2008;88:1089–118.
[47] Li L, Lei Q, Zhang S, et al. Screening and identification of key biomarkers in hepatocellular carcinoma: evidence from bioinformatic analysis. Oncol Rep. 2017;38:2607–18.
[48] Xu F, Guan Y, Xue L, et al. The effect of a novel glycolysis-related gene signature on progression, prognosis and immune microenvironment of renal cell carcinoma. BMC Cancer. 2020;20:1207.
[49] Tomita Y, Yuno A, Tsukamoto H, et al. Identification of promiscuous KIF20A long peptides bearing both CD4+ and CD8+ T-cell epitopes: KIF20A-specific CD4+ T-cell immunity in patients with malignant tumor. Clin Cancer Res. 2013;19:4508–20.
[50] Xie F, He C, Gao S, et al. KIF20A silence inhibits the migration, invasion and proliferation of non-small cell lung cancer and regulates the JNK pathway. Clin Exp Pharmacol Physiol. 2020;47:135–42.
[51] Liu SL, Lin HX, Qiu F, et al. Overexpression of Kinesin family member 20A correlates with disease progression and poor prognosis in human nasopharyngeal cancer: a retrospective analysis of 105 patients. PLoS One. 2017;12:e0169280.
[52] Xiong M, Zhuang K, Luo Y, et al. KIF20A promotes cellular malignant behavior and enhances resistance to chemotherapy in colorectal cancer through regulation of the JAK/STAT3 signaling pathway. Aging (Albany NY). 2019;11:11905–21.
[53] Wu C, Qi X, Qiu Z, et al. Low expression of KIF20A suppresses cell proliferation, promotes chemosensitivity and is associated with better prognosis in HCC. Aging (Albany NY). 2021;13:22148–63.
[54] Zhang Z, Chai C, Shen T, et al. Aberrant KIF20A expression is associated with adverse clinical outcome and promotes tumor progression in prostate cancer. Dis Markers. 2019;2019:14782730–10.
[55] Jin Z, Tao S, Zhang C, et al. KIF20A promotes the development of fibrosarcoma via PI3K-Akt signaling pathway. Exp Cell Res. 2022;420:113322.